

ORIGINAL PAPER

T. Irifune · H. Naka · T. Sanehira · T. Inoue  
K. Funakoshi

## In situ X-ray observations of phase transitions in $\text{MgAl}_2\text{O}_4$ spinel to 40 GPa using multianvil apparatus with sintered diamond anvils

Received: 2 April 2002 / Accepted: 29 July 2002

**Abstract** Phase transitions in  $\text{MgAl}_2\text{O}_4$  spinel have been studied at pressures 22–38 GPa, and at temperatures up to 1600 °C, using a combination of synchrotron radiation and a multianvil apparatus with sintered diamond anvils. Spinel dissociated into a mixture of MgO plus  $\text{Al}_2\text{O}_3$  at pressures to 25 GPa, while it transformed to the  $\text{CaFe}_2\text{O}_4$  (calcium ferrite) structure at higher pressures via the metastably formed oxide mixture upon increasing temperature. Neither the  $\varepsilon$ -phase nor the  $\text{CaTi}_2\text{O}_4$ -type  $\text{MgAl}_2\text{O}_4$ , which were reported in earlier studies using the diamond-anvil cell, were observed in the present pressure and temperature range. The zero-pressure bulk modulus of the calcium-ferrite-type  $\text{MgAl}_2\text{O}_4$  was calculated as  $K = 213$  (3) GPa, which is significantly lower than that reported by Yutani et al. (1997), but is consistent with a more recent result by Funamori et al. (1998) and that estimated by an ab initio calculation by Catti (2001).

**Keywords** Spinel · Calcium ferrite · In situ X-ray diffraction · Phase transition · Sintered diamond anvil

### Introduction

$\text{MgAl}_2\text{O}_4$  spinel is an important rock-forming mineral, which constitutes peridotites originated from the uppermost part of the Earth's mantle. Phase transitions in  $\text{MgAl}_2\text{O}_4$  have been extensively studied, using

diamond-anvil cell and multianvil apparatus (Liu 1975, 1978; Ohtani et al. 1975; Irifune et al. 1991; Funamori et al. 1998; Catti 2001), as well as shock compression (Shäfer et al. 1983), because olivine transforms to this structure at high pressure, and the seeking of the post spinel phase was one of the most important subjects of the high-pressure mineral physics to address the mineralogy of the lower mantle. Studies of the phase transitions in  $\text{MgAl}_2\text{O}_4$  are also important to investigate the nature of the aluminous phase in the deeper parts of the mantle.

Spinel was found to decompose into an assemblage of MgO periclase +  $\text{Al}_2\text{O}_3$  corundum at pressures greater than about 15 GPa (Liu 1975, 1980; Ohtani et al. 1975), at a temperature close to 1000 °C, on the basis of high-pressure experiments and thermodynamic analyses. Akaogi et al. (1999) further studied this phase boundary precisely between 1200 and 1600 °C, and concluded that the boundary is expressed by an equation  $P$  (GPa) =  $12.3 + 0.0023 T$  (°C).

At higher pressures, above ~25 GPa, there have been some contradictory results on the nature of the phase transition and the properties of the high-pressure phases of spinel. Liu (1978) reported that the oxides recombine to form a new dense phase ( $\varepsilon$ - $\text{MgAl}_2\text{O}_4$ ) at 25 GPa, at ~1000 °C, whereas Irifune et al. (1991) demonstrated that a calcium-ferrite-type phase is stable under similar pressure and temperature conditions. The latter result was confirmed by Akaogi et al. (1999), where the transition from the oxide mixture to the calcium-ferrite phase was observed at 26–27 GPa, at temperatures 1400–1900 °C. Akaogi et al. (1999) also suggested that this boundary has a negative Clapeyron slope.

More recently, Funamori et al. (1998) studied the phase transitions in  $\text{MgAl}_2\text{O}_4$  at still higher pressures using a diamond-anvil cell. They also observed that spinel transforms to the calcium-ferrite phase, but it further transforms to a new phase possessing the  $\text{CaTi}_2\text{O}_4$  structure at pressures greater than 34–40 GPa, at temperatures of ~1700–2700 °C. As Funamori et al. (1998) did not clearly mention the pressure at which the transformation took place, and also because the

T. Irifune (✉) · H. Naka · T. Sanehira · T. Inoue  
Geodynamics Research Center, Ehime University  
Matsuyama 790-8577, Japan  
e-mail: irifune@dpc.ehime-u.ac.jp  
Fax: +81-89-9279640  
Tel.: +81-89-9279645

K. Funakoshi  
Japan Synchrotron Radiation Institute,  
1-1 Koto, Mikazuki-cho, Sayo-gun  
Hyogo 679-5198, Japan

temperature was only poorly defined in their study, more quantitative studies are required to clarify the nature of this phase transformation. They estimated a bulk modulus of about 210 GPa for both of these high-pressure forms of spinel, which is significantly lower than the earlier result for the calcium-ferrite phase [ $K_0 = 241$  (3) GPa] by Yutani et al. (1997). This disagreement should also be addressed with additional experimental data.

The pressures available in the multianvil apparatus at high temperature have been limited to about 25 GPa using conventional tungsten carbide anvils. The use of sintered diamond anvils in this apparatus, however, extended this limit to higher pressures of about 30 GPa (e.g. Kondo et al. 1993; Funamori et al. 1996; Oguri et al. 1998). Nevertheless, the size of commercially available anvil cubes and the capacity of the DIA-type multianvil apparatus suitable for the operation of such anvil assembly were limited to ~10 mm and ~500 tons, respectively, which hindered experiments at higher pressures.

Ito et al. (1998) used a combination of sintered diamond anvils of larger dimensions (14-mm edge length) and a specially designed oil chamber to operate the first-stage split-sphere anvils, and succeeded in producing pressures up to 38 GPa in a multianvil apparatus. They studied phase transitions in pyrope garnet, and demonstrated that it transforms to nearly pure aluminous perovskite at these pressures. However, the pressures in Ito et al. (1998) were estimated using a calibration curve based on the phase transitions in some reference materials at lower pressures and at room temperature, which accordingly should have significant uncertainties.

We have been working extensively to introduce the large sintered diamond anvils, such as adopted in quench experiments by Ito et al. (1998), for in situ X-ray observations using a DIA-type multianvil apparatus possessing a press capacity of 1500 ton (SPEED-1500; Utsumi et al. 1998) at SPring-8. In situ X-ray diffraction study is now possible at extended pressures to ~40 GPa, and we here report the results of such experiments on the phase transitions in  $\text{MgAl}_2\text{O}_4$  using this technique.

## Experimental

In situ X-ray observations under high pressure and temperature were conducted using SPEED-1500 at BL04B1, SPring-8, where intense white X-rays of synchrotron radiation is available. An X-ray beam with dimensions of  $50 \times 50 \mu\text{m}$  was directed to the sample via horizontal and vertical slits through the anvil gap of SPEED-1500. An energy-dispersive system with a pure Ge solid-state detector was used for X-ray diffraction measurements, together with a CCD camera for radiographic imaging of the sample. A 4096-channel analyzer was used to acquire photons in a range of 30–150 keV, which was carefully calibrated with characteristic X-ray lines of some reference metals, so that the precision of the energy measurements was about  $\pm 30$  eV per channel. The diffraction angle ( $2\theta$ ) was fixed to about  $6^\circ$ , which was also calibrated using known diffraction peaks of standard samples, such as MgO and Au, under ambient conditions. The uncertainty of the diffraction angle thus determined was typically  $\pm 0.002^\circ$  in each

measurement. Thus, the lattice parameters of a crystalline sample can be determined with an accuracy of about 0.1% of the nominal values in the present in situ X-ray diffraction measurements.

The cell assemblage used in the present in situ X-ray diffraction study is illustrated in Fig. 1. Sintered diamond cubes of 14 mm edge length and truncations of 1.5 mm ( $\text{TEL} = 1.5$ ), supplied by Sumitomo Electric Co. Ltd., were used as the second-stage anvils for the multianvil apparatus. Mo foils of 50- $\mu\text{m}$ -thick, cemented TiC sheets were used as the leads for electric power supply to twin Re sheet heaters 25  $\mu\text{m}$  thick. The pressure medium was made of sintered  $\text{LaCrO}_3$  except for the central part where the sample was placed; a sintered MgO disc with cemented amorphous boron rods for the X-ray window (in runs S312, S369 and S402; see following section) was used in this part, where the sample and the pressure marker were enclosed in a hole 0.8 mm in diameter. We used 1.5-mm-thick pyrophyllite circular gasket, as shown in Fig. 1, to realize homogeneous compression of the gasket-pressure medium system. The inner diameter of the gasket was fixed at 4.0 mm, but we used gaskets with various outer diameters of 12.0, 10.0 and 9.0 mm (i.e. the ring widths, indicated by  $W$  in Fig. 1, were 4.0, 3.0 and 2.5 mm) for runs S312, S369 and S402, respectively.

An  $\text{MgAl}_2\text{O}_4$  single crystal, the same sample as used in Irifune et al. (1991), was crushed and ground in a hardened ceramic mortar, and used as starting material for the present high-pressure experiments. Another sample used a mixture of powders of MgO and Au as pressure reference materials. In earlier runs (S244 and S246), we enclosed these two samples on both sides of the thermocouple junction. However, we noted that the anvil gap becomes narrower with increasing pressure down to 150–200  $\mu\text{m}$ , as displayed in Fig. 2, and it was hard to detect X-ray diffractions from both of the two samples; the size of the folded thermocouple became 50–100  $\mu\text{m}$  and it often moved towards one side upon compression, thus shading one of the samples from the X-ray beam and interfering with the diffraction of the sample. So in later experiments (S312, S369, S402), we mixed a powder of spinel with that of gold (5:1 in weight), which was sintered in an oven for 24 h at 1000  $^\circ\text{C}$  prior to the run, and used as the sample for in situ X-ray observations. Two such sample rods were placed in the upper and the lower parts of the MgO container in these runs. No reactions between the sample spinel and the surrounding MgO pressure medium were recognized by electron microprobe analyses of the sample charge after the run.

Temperature was measured using a pair of  $\text{W}_{97}\text{Re}_3$  and  $\text{W}_{75}\text{Re}_{25}$  thermocouple wires of 50  $\mu\text{m}$  in diameter, whose cold junction was placed on the surface of the sintered diamond anvils via a pair of thicker (100  $\mu\text{m}$ ) wires (Fig. 2). The temperature at the

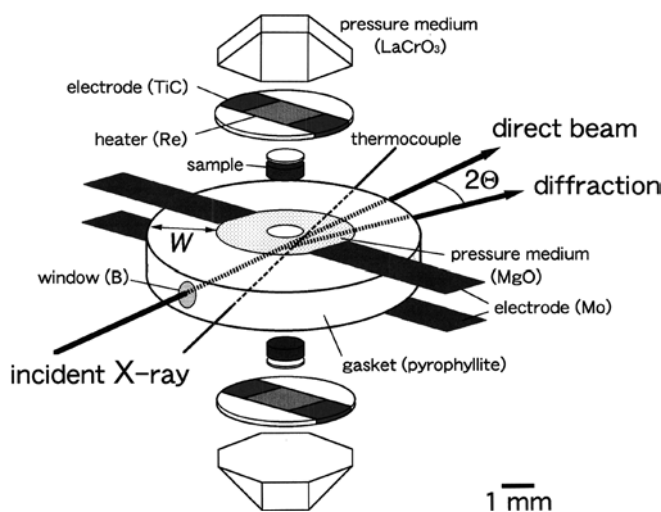


**Fig. 1** An illustration of the cell assembly used for in situ X-ray diffraction measurements using sintered diamond anvils.  $W$  Width of a circular pyrophyllite gasket

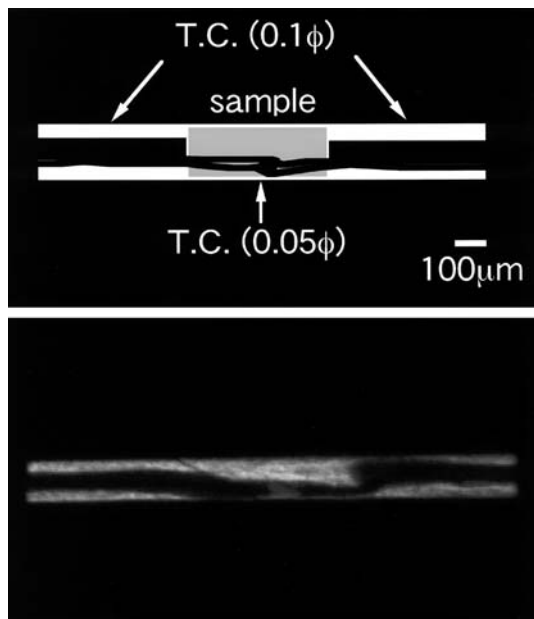


**Fig. 2** A CCD image (*below*) of the sample and the thermocouple under pressure (run S246, at about 25 GPa), and the schematic illustration (*above*). As the anvil gap, which was initially 1.5 mm, became narrower with increasing pressure, only one side of the two samples, which sandwiched the thermocouple hot junction, was observed by X-ray diffraction

anvil surface was measured by an additional thermocouple, which was used to correct the nominal temperature. Fluctuation of temperature was within  $\pm 5$  °C throughout the run, and the effect of temperature gradients within the sample on the temperature measurement may be of the order of  $\pm 20$  °C, as discussed in Kuroda et al. (2000) and Irifune (2002). However, the pressure effects on the thermocouple emf was not taken into consideration in the present study, as is the case in most multianvil experiments; a linear extrapolation using the pressure effects measured at lower pressures (e.g. Mao and Bell 1971) suggests that these temperatures may be underestimated by  $\sim 100$  °C at the present pressure/temperature range. In some runs, thermocouple failure occurred during compression or heating, and the temperatures in these runs were estimated based on a relationship between supplied electric power and temperature in successful runs.

The pressures in the present in situ X-ray observations were estimated on the basis of an equation of state of gold by Anderson et al. (1989). In some cases, where the diffraction peaks of gold were not available for accurate unit-cell volume measurements, the pressure was calculated using an equation of state of MgO by Jamieson et al. (1982), which is known to provide pressures virtually identical to those based on Anderson's gold scale (e.g. Funamori et al. 1996).

Funamori et al. (1996) made a comparison between existing pressure scales based on the equations of state of NaCl, Au and MgO, and concluded that the Anderson's gold scale agreed reasonably with Decker's NaCl scale (Decker 1971). This latter scale has been used at pressures to  $\sim 25$  GPa and temperatures to  $\sim 1000$  °C as the most reliable pressure standard, but is unsuitable at higher pressure/temperature conditions because of the phase transition to the CsCl structure and/or significant crystal growth at high temperature. On the other hand, Hirose et al. (2001a,b) also made comprehensive comparison of the Anderson scale with other pressure scales, such as Pt, Mo and W, and demonstrated that this scale gives slightly ( $\sim 0.5$  GPa) higher pressures than most of the others.

In the present X-ray in situ measurements, the press load was applied first to the desired values up to 900 tons, and then

temperature was gradually increased to 1000 °C in about 30 min. In the course of this, X-ray diffraction data were acquired every 200–300 °C for about 5 min. Then the temperature was increased more slowly to 1500–1600 °C over about 1–2 h, and the X-ray diffraction measurements were made every 100–200 °C at this stage where the temperature was maintained for about 10 min. At the highest temperature, heating was conducted for longer durations up to about 2 h, and the X-ray diffraction data were acquired several times for 5–10 min during this period. The phases present under each  $P$ – $T$  condition were identified from the observed diffraction patterns, and the unit-cell volumes of the sample and the pressure marker were determined. Then the run was quenched to room temperature, and the pressure was released very slowly over 2 days. The recovered sample was polished and further examined by X-ray powder diffraction and electron microprobe analyses.

Some quench experiments were also conducted to confirm the stability of phases and to define the phase boundary between the high-pressure phases of spinel, using a cell assembly similar to that used in the in situ X-ray observations. Runs were made at pressures of 24–26 GPa and at temperatures of 1000–1400 °C with a DIA-type multianvil apparatus (ORANGE-1000) at GRC, Ehime University. The heating duration was typically 30–60 min, but 5 h in runs at 1000 °C. The pressure calibration in the quench experiments was made on the basis of the results of the present in situ X-ray diffraction experiments. We observed that the phase boundary between the oxides and the calcium-ferrite phase was located at 25 GPa, 1600 °C by the in situ measurements, which were used as the pressure reference point for the present quench experiments so that the pressures become mutually consistent between these two types of experiments. The recovered samples in the quench experiments were also examined by X-ray diffraction and electron-microprobe measurements.

## Results

Five in situ X-ray diffraction measurements were conducted at pressures of 22–38 GPa, at temperatures up to 1600 °C. Table 1 lists the pressure at the highest temperature for each run, and the heating duration under such a  $P$ – $T$  condition. The results in this table represent the phases present at the final stage of the heating under pressure, immediately before quenching. S244 and S246 were conducted with tungsten carbide anvils, while S312, S369 and S402 were made using sintered diamond anvils. The temperatures for the runs S244, S369 and S402 were estimated from the supplied power because of thermocouple failure, and accordingly may suffer an uncertainty of the order of  $\pm 100$  °C. Details of these runs are summarized as follows.

### S244

In this run, we placed a pure  $\text{MgAl}_2\text{O}_4$  spinel sample and the pressure marker of  $\text{MgO} + \text{Au}$  into the  $\text{MgO}$  pressure medium. Some selected X-ray diffraction patterns of the spinel sample are depicted in Fig. 3A. Both the sample and the pressure marker were clearly seen with a CCD camera throughout the run, and the pressures were determined by the unit-cell volume changes of Au. However, we were unable to remove the diffraction lines from the surrounding  $\text{MgO}$  pressure medium (e.g. Fig. 3A,a), because we did not use the amorphous B window in this and the next (S246) run. We also

**Table 1** Experimental conditions and the results. *Per* MgO periclase; *Cor* Al<sub>2</sub>O<sub>3</sub> corundum; *CF* calcium ferrite type MgAl<sub>2</sub>O<sub>4</sub>; *tr.* trace

Run no.	Pressure (GPa)	Temperature (°C)	Heating time (min)	Results
In situ X-ray diffraction measurements				
S244	22.1	1500 <sup>a</sup>	70	Per + Cor
S246	25.0	1600	10	Per + Cor + tr. (CF)
S312	30.9	1500	40	CF
S369	34.4	1500 <sup>a</sup>	135	CF
S402	36.3	1600 <sup>a</sup>	10	CF
Quench experiments				
OD206	25.9	1000	300	Per + Cor
OD125	26.2	1000	300	CF + tr. (Per + Cor)
OD198	25.8	1100	60	Per + Cor
OD197	25.1	1200	60	Per + Cor
OD110	26.0	1200	60	CF + tr. (Per + Cor)
OD195	24.1	1400	30	Per + Cor
OD202	25.5	1400	30	Per + Cor + tr. (CF)
OD102	25.8	1400	30	CF

<sup>a</sup> Thermocouple failure occurred in the course of increasing pressure or temperature, and the temperature was estimated from supplied electric power. *P* and *T* conditions and the results of in situ X-ray diffraction measurements are those at the final stage of heating prior to quenching

observed the diffraction lines from the W-Re thermocouple in this run on the spinel side.

Pressure was increased to about 27 GPa at room temperature, where we observed broader diffraction peaks of spinel (Fig. 3A,b), which started to dissociate into an assemblage of periclase and corundum at 800 °C and at a pressure of 24.7 GPa (Fig. 3A,c). At temperatures higher than 1000 °C and at pressures of about 22–24 GPa, spinel completely dissociated into the oxides (Fig. 3A,d,e). No other phases were observed after about 70 min at 22.1–22.4 GPa, at 1500 °C.

#### S246

The pressure was increased to about 30 GPa at room temperature in this run (Fig. 3B,a,b). We were unable to see the pressure marker side with a CCD camera and only very few diffraction lines of Au were identified, as the hot junction of the thermocouple slightly (~50 μm) moved to one side upon compression and also the anvil gap became smaller with increasing pressure (see Fig. 2) as compared with that of run S244. Thus, the pressures of this run were estimated from the few minor peaks of Au and MgO, which were seen in the diffraction patterns of the sample side. As most of these peaks overlapped with those of the sample, particularly at temperatures below 800 °C (Fig. 3B,b,c), the pressures had relatively large uncertainties of ~± 1 GPa under these conditions. Nevertheless, we were able to determine the pressure with reasonable precision (± 0.3 GPa) at higher temperatures, because the diffraction peaks became sharper and were well resolved, and also because some additional diffraction peaks of MgO produced by the

dissociation of spinel were available for pressure calculations at these temperatures (Fig. 3B,d,e).

The overall nature of the phase change with increasing temperature in this run was similar to that of S244, but a few minor diffraction lines, which correspond to those of the calcium-ferrite structure, were observed at 1600 °C, at 25 GPa. The presence of a small amount of the calcium-ferrite phase was also confirmed in the quenched sample using microfocus X-ray diffractometry, which suggests that this pressure and temperature condition is close to the phase boundary between the oxide mixture and the calcium-ferrite phase.

#### S312 and S369

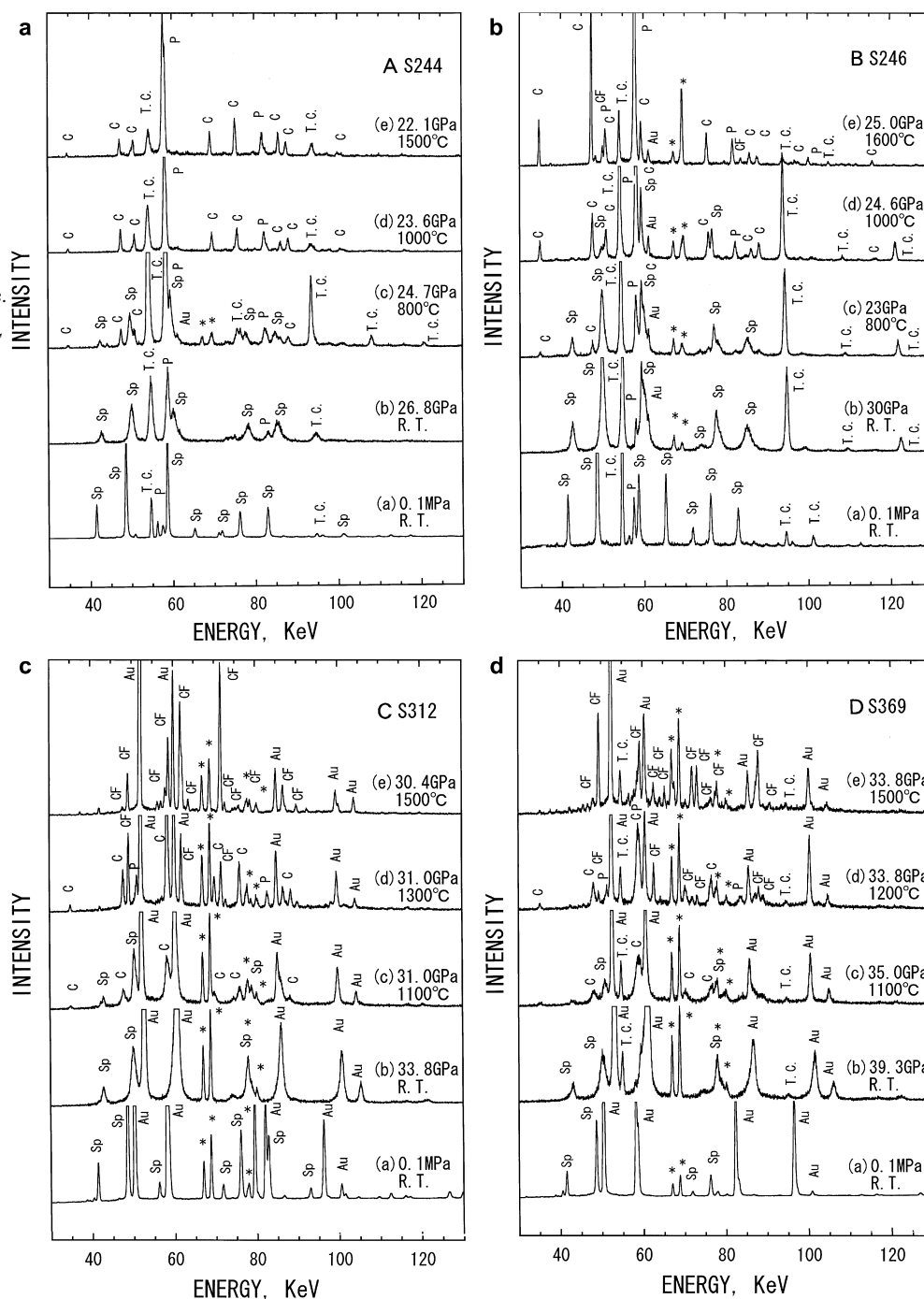
As it was difficult to measure the X-ray diffractions from both the sample and the pressure marker in the previous two runs, we used a mixture of spinel and gold powders as the starting material in these and subsequent runs. We also adopted amorphous boron rod windows, which were placed before and behind the sample through the MgO pressure medium and pyrophyllite gasket along the X-ray path (Fig. 1), to avoid the diffraction peaks of the surrounding MgO medium. Thus, we did not see any peaks of MgO under ambient conditions (Fig. 3C,a, and D,a) and at high pressures to about 34 GPa (Fig. 3C,b) for S312 and 39 GPa (Fig. 3D,b) and for S369, respectively, which is in contrast to the two earlier runs.

In runs S312 and S369, spinel partially decomposed to MgO + Al<sub>2</sub>O<sub>3</sub> at about 900–1100 °C, at pressures of 31–35 GPa (Fig. 3C,c and D,c). Then the calcium-ferrite phase appeared with further increasing temperature to 1200–1300 °C (Fig. 3C,d and D,d). Virtually a single phase (plus Au) of the calcium-ferrite type MgAl<sub>2</sub>O<sub>4</sub> was observed at pressures of 30.4–30.9 GPa (Fig. 3C,e) and 33.8–34.4 GPa (Fig. 3D,e), at a temperature of 1500 °C. Heating at this temperature was maintained for 40 min (S312) and 135 min (S369), but no further phase transitions were observed.

#### S402

In this run, the highest pressure of about 41 GPa was achieved at room temperature, but it decreased to 36–38 GPa upon heating. The nature of the phase transition in spinel was similar to those observed in S312 and S369; spinel transformed to the calcium-ferrite structure via the oxide mixture with increasing temperature (Fig. 3E,a–d). In this run, however, we obtained relatively poor diffraction peaks of the sample, mainly because of a significant reduction of the anvil gap at this pressure. Moreover, the heater became unstable after heating for a few minutes at the highest temperature of 1600 °C, and we only obtained diffraction profiles of poor quality particularly at this temperature (Fig. 3E,e). Thus, it was hard to unequivocally identify the phases present from the in situ X-ray diffraction pattern alone.

**Fig. 3A–E** Variations of the X-ray diffraction profiles of spinel as a function of pressure and temperature. S244 (A) and S246 (B) were conducted with conventional tungsten carbide anvils, while sintered diamond anvils were used in other runs, S312 (C), S369 (D) and S402 (E). In these runs, pressure was applied first and then the temperature was increased gradually, and heating was maintained for 10–135 min at the highest temperature. *Sp* MgAl<sub>2</sub>O<sub>4</sub> spinel; *P* MgO periclase; *T.C.* W–Re thermocouple; *C* Al<sub>2</sub>O<sub>3</sub> corundum; *Au* gold; *CF* calcium-ferrite-type MgAl<sub>2</sub>O<sub>4</sub>; asterisk characteristic lines of Au



Nevertheless, microfocus X-ray diffraction analyses demonstrated that only the calcium-ferrite phase existed in the quenched sample. Thus, it is unlikely that the CaTi<sub>2</sub>O<sub>4</sub> phase reported by Funamori et al. (1998) was formed under these conditions, as this phase was reported to be quenchable under ambient conditions.

#### Quench experiments

Table 1 lists *P–T* conditions and the results of the quench experiments using MgAl<sub>2</sub>O<sub>4</sub> spinel starting

material and tungsten carbide anvils. We observed the formation of either the assemblage of MgO + Al<sub>2</sub>O<sub>3</sub> or the calcium-ferrite phase at pressures of 24–26 GPa, and at a temperature of 1000–1400 °C. No evidence of the formation of other phases, including the  $\epsilon$ -MgAl<sub>2</sub>O<sub>4</sub> or CaTi<sub>2</sub>O<sub>4</sub> phases was obtained under these conditions. The boundary between these two phases is likely to have a negative Clapeyron slope, which is consistent with the result of Akaogi et al. (1999). However, the phase transition pressures of our study are substantially lower than those of Akaogi et al. (1999).

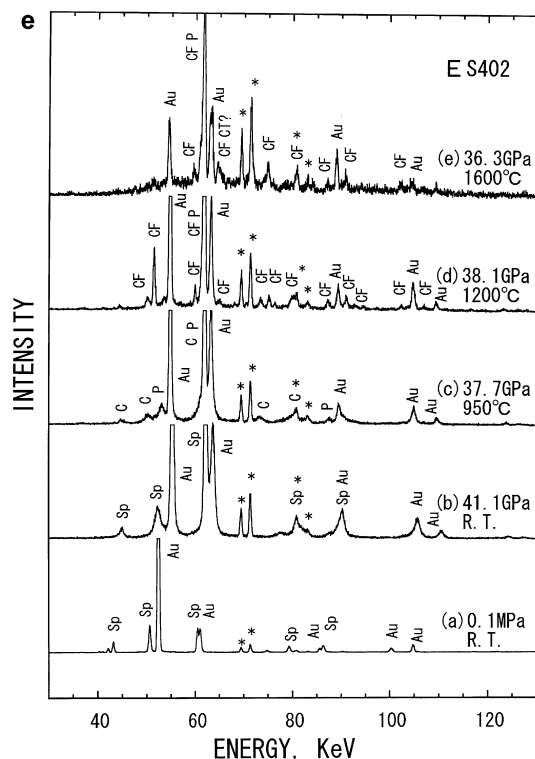


Fig. 3a-e (Continued)

We did not make any reversal experiments, because it is quite difficult to synthesize the calcium-ferrite phase sufficiently for such purposes at these pressures. So the assemblage of periclase and corundum at relatively low temperatures of 1000–1100 °C could have been formed metastably, as demonstrated in our in situ X-ray measurements described above. Thus, there is some possibility that the boundary at these lower temperatures may be overestimated, but the consistency of the Clapeyron slope between our results and those of Akaogi et al. (1999) at higher temperatures of 1400–1900 °C and the significantly longer run durations (1 and 5 h for the runs at 1100 and 1000 °C, respectively) adopted in the present quench experiments as compared with those (5–10 min) at the corresponding temperatures for the in situ measurements suggest that our experiments were also close to those in chemical equilibrium.

## Discussion

### High-pressure generation using sintered diamond anvils

Three in situ X-ray diffraction experiments with sintered diamond anvils have been conducted using the spinel starting material and essentially the same cell assemblage except for the size of the circular gaskets. Figure 4 shows the pressure changes in these three runs with changing press load. The efficiency of pressure generation depends largely on the gasket width ( $W$ ), and pressures up to about 41 GPa were produced when we

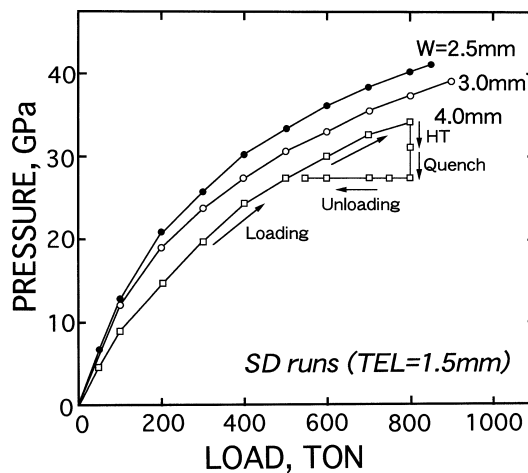


Fig. 4 Pressure versus press load for sintered diamond runs with various gasket width ( $W$ ). Generation of pressures of ~40 GPa without blowout is possible when we adopt the smallest gasket size ( $W = 2.5$  mm) in the present cell assembly. The pressure generally dropped with increasing temperature (*HT*), and further decreased upon quenching, as demonstrated for the case of  $W = 4.0$  mm. The pressure does not decrease effectively in the unloading process until the pressure load reaches 100–200 tons, where the blowout frequently occurs after heating at 600–900 tons

adopt the smallest size of  $W = 2.5$  mm at a press load of 850 tons. Further higher pressures can be produced if we adopt gaskets of smaller size, but our experience shows that the chances of blowout also increase when we use such small gaskets. Thus, we used this size ( $W = 2.5$  mm) for the standard gasket in other experiments up to 40 GPa for safety, as the blowout often causes serious damage to both sintered diamond-anvil cubes and the first-stage tungsten carbide anvils.

In these three runs and the subsequent runs with sintered diamond anvils for other studies, we had no blowouts in the course of compression and during heating, but the occurrence of blowout upon releasing pressure, particularly after heating above 600 tons, was almost inevitable. This is likely to be caused, at least partly, by an uneven decompression of the second-stage anvils due to significant deformation of the guide blocks of conventional DIA-type apparatus under pressure, as discussed in Irifune (2002). Nevertheless, the blowout on release of pressure generally occurs at relatively low-press loads of ~100–200 tons, until which the pressures inside the pressure medium are essentially unchanged (see Fig. 4), which does not necessarily cause any serious damage to the anvils, so that the sintered diamond anvils could be repeatedly used for subsequent experiments.

The heating system of the present cell assemblage performs well at least up to about 1500–1600 °C, but occasionally had thermocouple failure, especially at press loads greater than ~600 tons, which led to some uncertainty in the temperature measurements. Moreover, the pressures dropped significantly upon heating to these temperatures, and such a pressure loss reached about 10% of the nominal pressures at room temperature (Fig. 4). Thus, we need further development of the

high-pressure cell to produce higher pressures at high temperatures. The improvements in design, size and materials for the gaskets are also a key to access higher pressures in multi-anvil apparatus, utilizing the potential of sintered diamond anvils.

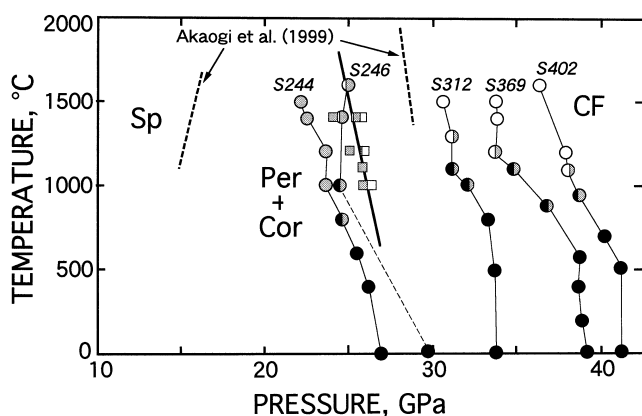
### Phase relations

Figure 5 depicts the results of the present in situ X-ray diffraction and quench experiments. Also shown are the results of recent quench experiments on the phase boundaries among spinel, oxide mixture and the calcium-ferrite phase by Akaogi et al. (1999). It was shown by in situ X-ray observations that spinel starting material first transforms to  $\text{MgO} + \text{Al}_2\text{O}_3$  at pressures of 30–40 GPa with increasing temperature, at about 1000 °C. However, the results of the present quench experiments demonstrated that spinel completely transforms to the calcium-ferrite structure at about 26 GPa, at a temperature of 1000 °C after a longer heating duration of about 5 h. Thus, these oxides observed in the in situ X-ray diffraction are most likely to have been metastably formed in the course of increasing temperature in the stability field of the calcium-ferrite phase.

The metastable formation of the intermediate phase was also noted in our earlier in situ X-ray experiments on the spinel–postspinel transition in  $\text{Mg}_2\text{SiO}_4$  and the ilmenite–perovskite transition in  $\text{MgSiO}_3$ . We observed the formation of the spinel phase from  $\text{Mg}_2\text{SiO}_4$  olivine starting material upon increasing the temperature to 1000 °C in the stability field of the postspinel phase (Irifune et al. 1998), while the tentative formation of the

ilmenite phase was also observed in the perovskite stability field when  $\text{MgSiO}_3$  enstatite was heated to similar temperatures (Kuroda et al. 2000). It seems that the metastable formation of an intermediate phase is a rather general phenomenon which occurs upon heating a low-pressure phase in the stability field of a high-pressure phase, when the phase transition occurs successively to the high-pressure phase via the intermediate phase. Thus, we should be careful in the determination of the phase boundary in limited heating durations of in situ X-ray diffraction measurements, as the formation of such metastable lower-pressure phases may lead to overestimation of phase-boundary pressures at such relatively low temperatures of ~1000 °C.

The results of our quench experiments and those based on in situ X-ray diffraction indicate that the calcium-ferrite phase is the only stable phase of  $\text{MgAl}_2\text{O}_4$  at pressures of 25–38 GPa and temperatures of 1000–1600 °C, as seen in Fig. 5. We saw no sign of formation of the  $\epsilon$ - $\text{MgAl}_2\text{O}_4$  reported by Liu (1978) under these conditions, which is consistent with Irifune et al. (1991), Funamori et al. (1998) and Akaogi et al. (1999), suggesting that this phase could have been metastably formed or is stable only at temperatures exceeding 2000 °C, as the temperature measurements in the diamond-anvil cell were not very accurate at that time. The presence of the  $\text{CaTi}_2\text{O}_4$  phase, which was formed at pressures greater than ~34 GPa and temperatures of about 1700–2700 °C by Funamori et al. (1998), was also not confirmed in the present in situ X-ray observations up to about 36–38 GPa, at temperatures of 1200–1600 °C. Thus, this phase may be stable at still higher pressures at these temperatures, and further studies at higher pressure are needed to determine the phase relations between  $\text{CaFe}_2\text{O}_4$  and  $\text{CaTi}_2\text{O}_4$  phases.



**Fig. 5** Conditions and the results of in situ X-ray diffraction (shown as circles) and quench (shown as squares) experiments on the  $\text{MgAl}_2\text{O}_4$  composition. Spinel (solid) persisted to ~1000 °C, where it first decomposed into periclase and corundum (shadow) even in the stability field of the calcium-ferrite phase (open) at pressures above 30 GPa. The results of the quench experiments with longer run duration indicate that the boundary between the oxide mixture and the calcium-ferrite phase locates at about 25–26 GPa, with slightly negative Clapeyron slope. The dashed lines are the boundaries determined by Akaogi et al. (1999) based on quench experiments

The present quench experiments demonstrated that the phase boundary between  $\text{MgO}$  periclase +  $\text{Al}_2\text{O}_3$  corundum and the calcium-ferrite phase has a negative slope ( $dP/dT$ ) of about  $-0.002 \text{ GPa}/^\circ\text{C}$ , which is consistent with the result of Akaogi et al. (1999). However, the boundary shifts toward lower pressures by about 2 GPa in the present study, as compared with those of Akaogi et al. (1999), where the boundary is constrained at temperatures between 1400 and 1900 °C (cf. 1000–1400 °C in the present study). The difference in phase-boundary pressures of this magnitude between the results based on in situ X-ray and quench experiments has also been reported in other phase transitions, such as spinel–postspinel in  $\text{Mg}_2\text{SiO}_4$  (Ito and Takahashi 1989; Irifune et al. 1998), ilmenite–perovskite in  $\text{MgSiO}_3$  (Ito and Takahashi 1989; Kuroda et al. 2000; Ono et al. 2001a), and garnet–aluminous perovskite + corundum in  $\text{Mg}_3\text{Al}_2\text{Si}_3\text{O}_{12}$  (Irifune et al. 1996; Hirose et al. 2001a,b). Such discrepancy is most likely to be caused by the systematic difference in the current measurements of pressures in conventional quench experiments based on the pressure calibration curves and those in the in situ

X-ray diffraction observations, as discussed by Hirose et al. (2001a, b).

The validity of the pressure reference material for in situ X-ray diffraction studies at pressures above ~25 GPa and at temperatures exceeding ~1000 °C has been a matter of debate (e.g. Kato et al. 1995; Funamori et al. 1996; Hirose et al. 2001a,b; Shim et al. 2001). As described earlier and also discussed in Irifune (2002), although Anderson's gold scale appears to be the most feasible pressure scale for in situ X-ray diffraction studies using the multianvil apparatus, there is a possibility that it may underestimate the pressures by 1–2 GPa at these pressures and temperatures as pointed out by Matsui et al. (2002). Thus, further refinement of the pressure scale for in situ X-ray measurement is required to address the possible cause of the slight discrepancy in the phase-transition pressures between Akaogi et al. (1999) and the present study.

### Bulk modulus of the calcium-ferrite phase and some implications

We determined the unit-cell volume of the calcium-ferrite phase after quenching under pressure. The pressure slightly decreased upon quenching, and we obtained volume data at 27.4 GPa [S312;  $V = 216.1(3) \text{ \AA}^3$ ; cf.  $V_0 = 240.7(3) \text{ \AA}^3$ ], 32.1 GPa [S369;  $V = 213.3(4) \text{ \AA}^3$  cf.  $V_0 = 240.0(2) \text{ \AA}^3$ ] and 34.7 GPa [S402;  $V = 213.1(7) \text{ \AA}^3$ ; cf.  $V_0 = 241.0(3) \text{ \AA}^3$ ]. An example of the results of the X-ray diffraction refinements is shown in Table 2. As the diffraction and characteristic X-ray peaks of gold and tungsten, as well as the diffraction peaks of the surrounding MgO, overlapped with some of the calcium-ferrite phase after quenching, relatively small numbers of diffraction peaks were unambiguously identified and used for the lattice-parameter refinements. Particularly, only five diffraction peaks were used in the measurements for the run S402, which accordingly resulted in larger uncertainties. Nevertheless, the unit-cell volumes de-

**Table 2** An example of the X-ray diffraction data of calcium-ferrite-type  $\text{MgAl}_2\text{O}_4$  quenched to room temperature under pressure (S312; 27.4 GPa). The obtained lattice parameters are;  $a = 8.327(5) \text{ \AA}$ ;  $b = 9.623(4) \text{ \AA}$ ;  $c = 2.696(2) \text{ \AA}$ ;  $V = 216.1(3) \text{ \AA}^3$ ; [cf.  $V_0 = 240.7(3) \text{ \AA}^3$ ]

$(h k l)$	$d_{\text{obs}}(\text{\AA})$	$d_{\text{cal}}(\text{\AA})$	$(d_{\text{obs}}/d_{\text{cal}})^{-1}$
0 4 0	2.4048	2.4057	-0.0004
3 2 0	2.4048	2.4044	-0.0002
1 2 1	2.2636	2.2640	-0.0002
1 3 1	2.0039	2.0033	0.0003
4 2 0	1.9097	1.9107	-0.0005
2 4 1	1.6488	1.6484	0.0003
4 0 1	1.6486	1.6478	0.0005
4 1 1	1.6235	1.6242	-0.0004
2 6 0	1.4972	1.4966	0.0004
1 6 1	1.3588	1.3599	-0.0008
2 6 1	1.3091	1.3085	0.0004

rived by these diffraction data were mutually consistent, although that of S402 shows a slightly larger value, as seen in Fig. 6.

Because thermocouple failure occurred in two runs (S369 and S402) out of three in situ X-ray diffraction measurements where we observed the formation of single phase of the calcium ferrite phase, we were unable to effectively constrain thermal expansivity of this phase under pressure. However, it is expected that the deviatoric stresses were relaxed during heating at 1500–1600 °C in these experiments, which should lead to unit-cell volume data under quasi-hydrostatic pressure at room temperature after cooling (e.g. Wang et al. 1996). Thus, the present unit-cell volume data on the quenched samples under pressure can be used for the determination of the room-temperature bulk modulus of the calcium-ferrite phase.

The zero-pressure volumes ( $V_0$ ) of these samples were measured using a laboratory microfocus X-ray diffractometer, as no synchrotron beam was available after the release of pressure because of the limited beamtime. The averaged value of these volumes was  $V_0 = 240.6(3) \text{ \AA}^3$ , which is slightly larger than those reported in earlier studies [ $V_0 = 240.00(15) \text{ \AA}^3$ , Irifune et al. 1991;  $V_0 = 240.3(2) \text{ \AA}^3$ , Funamori et al. 1998], but is almost within the uncertainties in these studies. A compression curve of this phase was then derived, using these volume data under pressure and the averaged zero-pressure volume, as depicted in Fig. 6. A third-order Birch–Murghnahan equation of state was used for least-squares fitting of the normalized volume data ( $V/V_0$ ), assuming  $dK/dP = 4$ . Thus determined zero-pressure bulk modulus ( $K_0$ ) of the calcium-ferrite phase was 213(3) GPa, which is significantly lower than the earlier result ( $K_0 = 241(3) \text{ GPa}$ ) by Yutani et al. (1997), but is close to the result by Funamori et al. (1998;  $K_0 = \sim 210 \text{ GPa}$ ).

Yutani et al. (1997) measured the unit-cell volume changes of the calcium ferrite phase synthesized in a

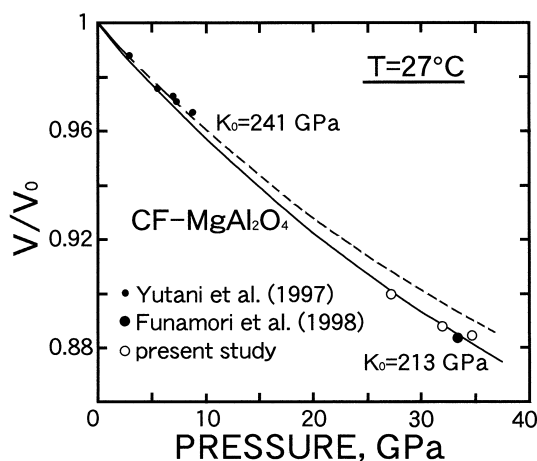


**Fig. 6** A room-temperature compression curve of the calcium-ferrite type  $\text{MgAl}_2\text{O}_4$  up to about 35 GPa determined by the present unit-cell volume data (open circles) using an equation of state. The volume data reported by Yutani et al. (1997) and that of Funamori et al. (1998) are also shown for comparison



multianvil apparatus by Irifune et al. (1991), using a combination of synchrotron radiation and diamond-anvil cell with a liquid pressure medium, at pressures up to 9 GPa at room temperature. However, their starting material was not the pure calcium-ferrite phase, but contained a significant amount of lower-pressure phases of periclase and corundum. In addition, the electron microprobe analysis by Irifune et al. (1991) suggests thus the calcium-ferrite phase used by Yutani et al. (1997) may have been somewhat non-stoichiometric. The use of such a sample could have yielded the bulk modulus, which was somewhat different from that of the calcium-ferrite phase possessing a pure  $\text{MgAl}_2\text{O}_4$  composition.

Recently, Catti (2001) made a theoretical study of stability, structure and compressibility of the high-pressure polymorphs of  $\text{MgAl}_2\text{O}_4$  spinel. Although this study focused on the nature of the  $\text{CaTi}_2\text{O}_4$  (Cmcm) phase, it suggests that the bulk modulus of the calcium-ferrite phase determined by Yutani et al. (1997) is overestimated, whereas that by Funamori et al. (1998) could be "slightly underestimated". The present result is thus quite consistent with such predictions based on an ab initio calculation.

The formation of an Al-rich phase with a structure related to that of calcium-ferrite has been reported in basaltic compositions under lower mantle conditions (Irifune and Ringwood 1993; Kesson et al. 1994; Hirose et al. 1999; Ono et al. 2001b). Irifune and Ringwood (1993) calculated the density changes in a basaltic composition on the basis of the experimental data to 28 GPa, assuming an arbitrary value for the bulk modulus of this Al-rich phase (i.e.  $K_0 = 200$  GPa), and concluded that the subducted oceanic crust may be denser than the surrounding mantle by 0.1–0.2  $\text{g cm}^{-3}$  in a limited depth interval of 660–800 km. This conclusion is further supported by recent studies at higher pressures, although the density crossover was confined in a smaller interval of less than 100 km immediately below the 660-km seismic discontinuity (Hirose et al. 1999; Ono et al. 2001b).

Ono et al. (2001b) showed that the proportion of the calcium-ferrite-type phase is about 20 vol% in a basaltic composition, and estimated that the density crossover occurs at depths of 660–730 km with a density contrast of up to 0.3  $\text{g cm}^{-3}$  using Yutani et al.'s bulk modulus for this phase. The present study shows that this value could be overestimated by more than 10%, which suggests that the density of the calcium-ferrite-type phase under lower-mantle conditions is underestimated in Ono et al. (2001b). However, the underestimation of the bulk density of the basaltic lithology is only about 0.01  $\text{g cm}^{-3}$  considering the volume proportion of the calcium-ferrite-type phase, which will not lead to any significant changes in the density contrast between the basaltic and the surrounding mantle compositions in the lower mantle.

The overestimation of the bulk modulus of  $\text{CaSiO}_3$  perovskite, a major constituent of the basaltic composition in the mantle transition region and the lower mantle (e.g. Irifune and Ringwood 1993), in earlier studies

(Mao et al. 1989; Tamai and Yagi 1989) has also been pointed out by Wang et al. (1996) and Shim et al. (2000), which should further increase the density of the subducted oceanic crust in the lower-mantle conditions. Moreover, the Al-rich phase by Irifune and Ringwood (1993) may not be of calcium-ferrite structure, but may possess a hexagonal symmetry, as suggested by Akaogi et al. (1999). Thus, further studies on the phase transitions and the  $P$ – $V$ – $T$  relations of the high-pressure phases in basaltic compositions are required to make more quantitative estimation of the density relationship between subducted oceanic crust and the surrounding mantle, and thereby to study the dynamics of the subducted slabs in the lower mantle, which may be conducted using the present technique with a combination of synchrotron radiation and multianvil apparatus.

**Acknowledgements** The authors thank Y. Higo, Y. Sueda, T. Ueda, Y. Tanimoto, A. Fukuyama, K. Ochi, F. Kurio and T. Kawahara for help in the in situ X-ray observations at SPring-8 (No: 2000A0061-CD-np and 2000B0093-ND-np). We also thank W. Utsumi, J. Ando and O. Shimomura for advice and encouragement during this study, and N. Funamori and an anonymous reviewer for comments on the article. The present study is partly supported by the grant-in-aid for Scientific Research (A) of the Ministry of Education, Science, Sport and Culture of the Japanese government (no: 11694088).

## References

- Akaogi M, Hamada Y, Suzuki T, Kobayashi M, Okada M (1999) High-pressure transitions in the system  $\text{MgAl}_2\text{O}_4$ – $\text{CaAl}_2\text{O}_4$ : a new hexagonal aluminous phase with implication for the lower mantle. *Phys Earth Planet Inter* 115: 67–77
- Anderson OL, Isaak DG, Yamamoto S (1989) Anharmonicity and the equation of state for gold. *J Appl Phys* 65: 1534–1543
- Catti M (2001) High-pressure stability, structure and compressibility of Cmcm– $\text{MgAl}_2\text{O}_4$ : an ab initio study. *Phys Chem Miner* 28: 729–736
- Decker DL (1971) High-pressure equation of state for NaCl, KCl, and CsCl. *J Appl Phys* 42: 3239–3244
- Funamori N, Yagi T, Utsumi W, Kondo T, Uchida T, Funamori M (1996) Thermoelastic properties of  $\text{MgSiO}_3$  perovskite determined by in situ X-ray observations up to 30 GPa and 2000 K. *J Geophys Res* 101: 8257–8269
- Funamori N, Jeanloz R, Nguyen JH, Kavner A, Caldwell WA, Fujino K, Miyajima N, Shinmei T, Tomioka N (1998) High-pressure transformations in  $\text{MgAl}_2\text{O}_4$ . *J Geophys Res* 103: 20813–20818
- Hirose K, Fei Y, Ma Y, Mao HK (1999) The fate of subducted basaltic crust in the Earth's lower mantle. *Nature* 397: 53–56
- Hirose K, Fei Y, Ono S, Yagi T, Funakoshi K (2001a) In situ measurements of the phase transition boundary in  $\text{Mg}_3\text{Al}_2\text{Si}_3\text{O}_{12}$ : implications for the nature of the seismic discontinuities in the Earth's mantle. *Earth Planet Sci Lett* 184: 567–573
- Hirose K, Komabayashi T, Murakami M, Funakoshi K (2001b) In situ measurements of the majorite–akimotoite–perovskite phase transition boundaries in  $\text{MgSiO}_3$ . *Geophys Res Lett* 28: 4351–4354
- Irifune T, Fujino K, Ohtani E (1991) A new high-pressure form of  $\text{MgAl}_2\text{O}_4$ . *Nature* 349: 409–411
- Irifune T, Ringwood AE (1993) Phase transformations in subducted oceanic crust and buoyancy relationships at depths of 600–800 km in the mantle. *Earth Planet Sci Lett* 117: 101–110
- Irifune T, Koizumi T, Ando J (1996) An experimental study of the garnet–perovskite transition in the system  $\text{MgSiO}_3$ – $\text{Mg}_3\text{Al}_2\text{Si}_3\text{O}_{12}$ . *Phys Earth Planet Inter* 96: 147–157

- Irifune T, Nishiyama N, Kuroda K, Inoue T, Isshiki M, Utsumi W, Funakoshi K, Urakawa S, Uchida T, Katsura T, Ohtaka O (1998) The postspinel phase boundary in  $\text{Mg}_2\text{SiO}_4$  determined by in situ X-ray diffraction. *Science* 279: 1698–1700
- Irifune T (2002) Application of synchrotron radiation and Kawai-type apparatus to various studies in high-pressure mineral physics. *Mineral Mag* (in press)
- Ito E, Takahashi E (1989) Post-spinel transition in the system  $\text{Mg}_2\text{SiO}_4$ – $\text{Fe}_2\text{SiO}_4$  and some geophysical implications. *J Geophys Res* 94: 10637–10646
- Ito E, Kubo A, Katsura T, Akaogi M, Fujita T (1998) High-pressure phase transition of pyrope ( $\text{Mg}_3\text{Al}_2\text{Si}_3\text{O}_{12}$ ) in a sintered diamond cubic anvil assembly. *Geophys Res Lett* 25: 821–824
- Jamieson JC, Fritz JN, Manghnani MH (1982) Pressure measurement at high temperature in X-ray diffraction studies: gold as a primary standard. In: Akimoto S, Manghnani MH (eds) *High-pressure research in geophysics*. Center for Academic Press, Tokyo, pp 27–48
- Kato T, Ohtani E, Morishima H, Yamazaki D, Suzuki A, Suto M, Kubo T (1995) In situ X-ray observation of high-pressure phase transitions of  $\text{MgSiO}_3$  and thermal expansion of  $\text{MgSiO}_3$  perovskite at 25 GPa by a double-stage multianvil system. *J Geophys Res* 100: 20475–20481
- Kesson SE, Fitz Gerald JD, Shelley JM (1994) Mineral chemistry and density of subducted basaltic crust at lower-mantle pressures. *Nature* 372: 767–769
- Kondo T, Sawamoto H, Yoneda A, Kato M, Matsumoto A, Yagi T (1993) Ultrahigh-pressure and high-temperature generation by use of the MA8 system with sintered-diamond anvils. *High Temp–High Press* 25: 105–112
- Kuroda K, Irifune T, Inoue T, Nishiyama N, Miyashita M, Funakoshi K, Utsumi W (2000) Determination of the phase boundary between ilmenite and perovskite in  $\text{MgSiO}_3$  by in situ X-ray diffraction and quench experiments. *Phys Chem Miner* 27: 523–532
- Liu LG (1975) Disproportionation of  $\text{MgAl}_2\text{O}_4$  spinel at high pressures and temperatures. *Geophys Res Lett* 2: 9–11
- Liu LG (1978) A new high-pressure phase of spinel. *Earth Planet Sci Lett* 41: 398–404
- Liu LG (1980) The equilibrium boundary of spinel = corundum + periclase: a calibration curve for pressures above 100 kbar. *High Temp–High Press* 12: 217–220
- Mao HK, Bell PM (1971) Behavior of thermocouples in the single-stage piston-cylinder apparatus. *Carnegie Inst Washington Yb* 69: 207–216
- Mao HK, Chen LC, Hemley RJ, Jephcoat AP, Wu Y (1989) Stability and equation of state of  $\text{CaSiO}_3$ -perovskite to 134 GPa. *J Geophys Res* 94: 17889–17894
- Matsui M, Nishiyama N, Cohen RE (2002) Comparison between the Au and MgO pressure calibration standards at high temperature. *Geophys Res Lett* (in press)
- Oguri K, Funamori N, Uchida T, Yagi T, Miyajima N, Fujino K (1998) High-pressure and high-temperature in situ X-ray diffraction study of natural garnet ( $\text{Mg}_{0.72}\text{Fe}_{0.17}\text{Ca}_{0.11}$ ) $_3\text{Al}_2\text{Si}_3\text{O}_{12}$  up to 32 GPa and 2000 K using MA8-type apparatus. *Rev High Press Sci Tech* 7: 59–61
- Ohtani E, Sawamoto H, Masaki K, Kumazawa M (1975) Decomposition of spinel  $\text{MgAl}_2\text{O}_4$  at extremely high pressure. In: Osugi J (ed) *Proc 4<sup>th</sup> Int Conf on High Pressure*. Kyoto, pp 185–189
- Ono S, Katsura T, Ito E, Kanzaki M, Yoneda A, Walter MJ, Urakawa S, Utsumi W, Funakoshi K (2001a) In situ observation of ilmenite–perovskite phase transition in  $\text{MgSiO}_3$  using synchrotron radiation. *Geophys Res Lett* 28: 835–838
- Ono S, Ito E, Katsura T (2001b) Mineralogy of subducted basaltic crust (MORB) from 25 to 37 GPa, and chemical heterogeneity of the lower mantle. *Earth Planet Sci Lett* 190: 57–63
- Schäfer H, Muller WF, Hornemann U (1983) Shock effects in  $\text{MgAl}_2\text{O}_4$ -spinel. *Phys Chem Miner* 9: 248–252
- Shim SH, Duffy TS, Shen G (2000) The equation of state of  $\text{CaSiO}_3$  perovskite to 108 GPa at 300 K. *Phys Earth Planet Inter* 120: 327–338
- Shim SH, Duffy TS, Shen G (2001) Evidence that the postspinel transition in  $\text{Mg}_2\text{SiO}_4$  is responsible for the 660-km seismic discontinuity. *Nature* 441: 571–574
- Tamai H, Yagi T (1989) High-pressure and high-temperature phase relations in  $\text{CaSiO}_3$  and  $\text{CaMgSi}_2\text{O}_6$  and elasticity of perovskite-type  $\text{CaSiO}_3$ . *Phys Earth Planet Inter* 54: 370–377
- Utsumi W, Funakoshi K, Urakawa S, Yamakata M, Tsuji K, Konishi H, Shimomura O (1998) SPring-8 beamline for high pressure science with multianvil apparatus. *Rev High Press Sci Tech* 7: 1484–1486
- Wang Y, Weidner DJ, Guyot F (1996) Thermal equation of state of  $\text{CaSiO}_3$  perovskite. *J Geophys Res* 101: 661–672
- Yutani M, Yagi T, Irifune T (1997) Compressibility of calcium ferrite-type  $\text{MgAl}_2\text{O}_4$ . *Phys Chem Miner* 24: 340–344